Theory of Y- and Comb-Shaped Polymer Brushes: The Parabolic Potential Framework

Inna Lebedeva, Ekaterina Zhulina, Frans A.M. Leermakers, Sergei Sheiko, Oleg Borisov

Theory of Y- and comb-shaped polymer brushes: the parabolic potential framework

Inna O.Lebedeva[1],Ekaterina B.Zhulina[2],Frans A.M.Leermakers[3], Sergei S.Sheiko[4], Oleg V. Borisov[1,2*]

[1]Institut des Sciences Analytiques et de Physico-Chimie pour l'Environnement et les Matériaux, UMR 5254 CNRS UPPA, 64053 Pau, France

[2]Institute of Macromolecular Compounds of the Russian Academy of Sciences, 199004 St.Petersburg, Russia

[3]Physical Chemistry and Soft Matter, Wageningen University, 6703 NB Wageningen, The Netherlands

[4] Department of Chemistry UNC, Chapel Hill, NC 27599-3290, USA

August 14, 2021

email: oleg.borisov@uiv-pau.fr

Abstract

The parabolic approximation for self-consistent molecular potential is widely used for theoretical analysis of conformational and thermodynamic properties of polymer brushes formed by linear or branched macromolecules. The architecture-dependent parameter of the potential (topological coefficient) can be calculated for arbitrary branched polymer architecture from the condition of elastic stress balance in all the branching points. However, the calculation routine for the topological coefficient does not allow unambigously identifying the range of applibility and the accuracy of the parabolic approximation. Here the limits of applicability of parabolic approximation are explored by means of numerical self-consistent field method for brushes formed by Y-shaped and comb-like polymers. We demonstrate that violation of the potential parabolic shape can be evidenced by appearance of multimodal distribution of the end monomer unit in the longest elastic path of the macromolecule. The asymmetry of branching of Y-shaped polymers does not disturb the parabolic shape of the potential as long as the degree of polymerization of the root segment remains sufficiently large. The same applies to comb-shape polymers with sufficiently long main chain and large number of branching points. For short comb-like polymers multiple modes in the distribution of the end monomer unit of the main chain are observed and related to deviation from the parabolic shape of the potential.

1 Introduction

Polymer brushes are formed by linear or branched macromolecules attached to an interface at high surface coverage assuring dominance of inter-molecular interactions. Solvated or solvent-free (dry) polymer brushes are used in technology and medicine for modification of adhesive, tribological, and biointeractive surface properties. Brush-like layers of biological macromolecules are found inside living species, e.g., cilia in lung airways and cell membranes.

Theoretical understanding of structure and properties of polymer brushes stem from pioneering works of Alexander[1] and de Gennes,[2] based on scaling approach which capture the most essencial structure-property relationships for brushes formed by linear chain polymers. More recent theoretical activity in this field amply exploited the strong-stretching (or quasi-classical) self-consistent field approximation suggested by Semenov[3] and further elaborated for solvated polymer brushes in refs[4,5] (see also a comprehensive review[6] on theory of polymer brushes).

According to the Semenov's approach[3] each chain is assimilated to the trajectory of a forward motion of a classical particle in the self-consistent potential field. The particle velocity is mapped to the local chain stretching. The non-uniform distribution of the local stretching along the contour of the chain assures minimum of its free energy in the potential field. Irrespectively of the chain free end position (starting point of any trajectory) the terminal segment of the chain reaches the grafting surface. As long as the chains exhibit linear (Gaussian) elasticity this condition of equal paths length (or eaqul "flight times") can be satisfied only if the potential has a parabolic shape. The condition of self-consistency requires that polymer density distribution dictated by the parabolic potential can be formed by an ensemble of non-equally and non-uniformly stretched chains without dead zones depleted of the chains free ends.

The equivalent arguments were further applied for brushes of tree-like macromolecules (dendrons) by Pickett who suggested that self-consistent molecular potential acting in brushes of tethered regular dendrons has also a parabolic shape.[7,8] These findings paved the way for generalization of the analytical self-consistent field approach to brushes of other architectures.[9–13] The parameters of the parabolic self-consistent potential can be calculated for an arbitrary tree-like or even cyclic macromolecules. However, this does not guarantee that a real self-consistent field potential has indeed the parabolic shape.

Notably, if the brush is formed by linear chain macromolecules, the self-consistent potential is parabolic only for stricktly monodisperse brushes. Even weak polydispersity of the brush-forming chains distores the parabolic

shape of the potential,[14,15] which is not always the case in brushes formed by branched macromolecules.[11]

The applicability of the parabolic potential approximation, i.e. the shape of the true self-consistent potential for any specific branched architecture of the brush-forming molecules can be verified by numerical self-consistent methods, that are free of any assumption about the stretching mode and do account for finite extensibility of the polymer chains.

The aim of the present paper is to explore the ranges of validity of the parabolic potential approximation for mono-component brushes formed by macromolecules with various branched architectures. In particular, we explore the simplest case of branched macromolecules, i.e. root-tethered Y-shaped macromolecules and further extend the analysis for comb-shape polymers tethered to planar surface. To establish applicability limits of this approach for various macromolecular architectures,we use the Scheutjens-Fleer numerical self-consistent field (SF-SCF) method.[16] Although quantitative predictions of the lattice-based SF-SCF theory concerning chain elasticity in the non-linear stretching regime do not exactly match results obtained within continuum models (see, e.g., discussion in recent review article[17]), this approach provides a robust tool for exploring both the shape of the self-consistent potential and the end-point distribution in brushes formed by branched macromolecules with varied architecture.

Notably, brushlike structures emerge as an outcome of self-assembly of copolymers comprising comb-shape blocks into diverse bulk morphologies. Such microphase segregated materials are being actively studied because of possibility to controll their optical and mechanical properties by tuning atchtectural parameters of constituent branched polymer blocks.[18–28]

The paper is organized as follows. In section 2 we present the general parabolic potential framework for arbitrary polymer architecture. In section 3 we employ numerical self-consistent field method to check range of applicability of the parabolic approximation to brushes of asymmetric Y-shaped polymers. In section 4 we extend our numerical analysis to brushes of comb-like polymers. In section 5 formulate the conclusions. In the Appendix we demonstrate how the parabolic potential can be derived explicitly for the brush formed by Y-shaped macromolecules.

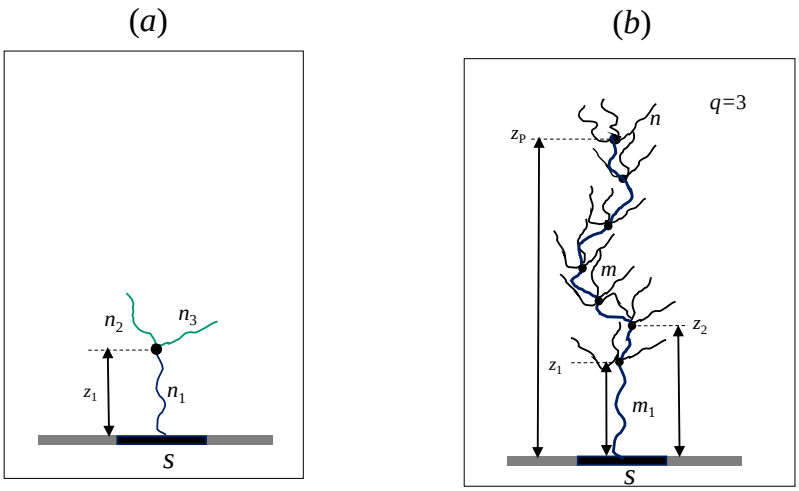

Figure 1: Schematic of Y-shape macromolecule (a) and comb-like polymer (b) tethered to the surface by the root segment of the main chain.

2 SS-SCF formalism.

According to previous studies,[7–13] the molecular potential $U(z)$ in the brush can be presented as

$$\frac{U(z)}{k_BT} = \frac{3}{2a^2}\kappa^2(H^2 - z^2) \tag{1}$$

where k_BT is the thermal energy, H is the brush thickness and κ is the topological coefficient. The latter has to be specified for each particular macromolecular architecture yet is remarkably independent of the grafting density and solvent quality. Eq 1 presumes the Gaussian (linear) elasticity of the tethered macromolecules on all length scales but can be generalized[6] for accounting finite chain extensibility. Crowding of the side chains near the branching points is not taken into account.

The values of κ for macromolecules with different architectures are calculated[11,13] by using the conditions of length conservation for the segments between branching units, and by balancing the elastic forces in all branching units of the macromolecule. For linear chains $\kappa_{lin} = \pi/2N$.[3]

The topological coefficient κ ensures conservation of number of monomer units in all linear segments of the molecule at any position of the free end-points. However, it does not ensure the absence of dead zones depleted of the free ends. Curvature of the grafting surface is known to produce dead zones in spherical and cylindrical convex brushes formed by both linear and branched polymers. Branching of the brush-forming macromolecules makes the free-end distribution more even, and may lead to virtual disappearance of the curvature-induced dead zones.[8,29] As demonstrated below, the dead zones, which are always present in the convex brushes, may appear even in planar brushes for some particular macromolecular architectures. In the case of the dead zone emergence, the parabolic potential, eq 1 is not a true self-consistent one.

The profile of free ends of the tethered macromolecules should be therefore checked for every specific chain architecture to identify the parameter space where the parabolic potential is valid. We use the numerical self-consistent method of Scheutjens and Fleer (SF-SCF) to examine distributions of the free ends.[16]

The molecular potential in eq 1 is related to the polymer density (volume fraction) profile $\phi(z)$ in the brush by a general equation

$$a^3\frac{\delta f\{\phi(z)\}}{\delta\phi(z)} = U(z) \tag{2}$$

where $f\{\phi(z)\}$ is the free energy density of monomer-monomer interactions. For non-ionic polymers, at $\phi(z) \ll 1$, it can be presented as a virial expansion

in powers of polymer volume fraction, that is

$$f\{\phi(z)\} = \upsilon\phi^2(z) + w\phi^3(z) + ... \tag{3}$$

where υa^3 and wa^6 are the second and the third virial coefficients of monomer-monomer interactions, respectively. The former is related to the Flory-Huggins polymer-solvent interaction parameter χ as $\upsilon = \frac{1}{2} - \chi$.

Under good ($\upsilon \gg w\phi$) or theta ($\mid \upsilon \mid \ll w\phi$) solvent conditions one can keep only the respective dominant term in the virial expansion. This leads to explicit expressions for the polymer density profile,

$$\phi(z) \approx \begin{cases} (3\kappa^2)/(4a^2\upsilon)(H^2 - z^2) & \upsilon \gg w\phi \\ \{(\kappa^2/2a^2w)(H^2 - z^2)\}^{1/2} & \mid \upsilon \mid \ll w\phi \\ -\upsilon/(2w) & \upsilon \leq 0, \mid \upsilon \mid \gg w\phi \end{cases} \tag{4}$$

Under good solvent conditions, according to eqs 2 and 3 there is a simple relation between self-consistent potential and polymer density profile, that is

$$\frac{U(z)}{k_BT} = 2\upsilon\phi(z)$$

and both have a parabolic shape. Through normalization of the polymer density profile,

$$\frac{s}{a^3}\int_0^H \phi(z)dz = N \tag{5}$$

one finds the brush thickness

$$H/a = \begin{cases} (2a^2\upsilon N/s\kappa^2)^{1/3} & \upsilon \gg w\phi \\ (2w)^{1/4}(4Na^2/\pi s\kappa)^{1/2} & \mid \upsilon \mid \ll w\phi \\ -2Nwa^2/(s\upsilon) & \upsilon \leq 0, \mid \upsilon \mid \gg w\phi \end{cases} \tag{6}$$

It is instructive to introduce the topological ratio

$$\eta = \frac{\kappa}{\kappa_{linear}} = \frac{2\kappa N}{\pi} \tag{7}$$

for brushes of branched polymers with the same number N of monomer units as in a linear macromolecule ($k_{linear} = \pi/(2N)$). The topological ratio quantifies a relative increase in the elastic free energy penalty for stretching of a branched macromolecule as compared to that for a linear one in a brush. The reduced thickness H/H_{linear} of the brush formed by branched macromolecules can be expressed as

$$\frac{H}{H_{linear}} = \begin{cases} \eta^{-1/3} & \upsilon \gg w\phi \\ \eta^{-1/2} & \mid \upsilon \mid \ll w\phi \\ \eta^0 & \upsilon \leq 0, \mid \upsilon \mid \gg w\phi \end{cases} \tag{8}$$

Free energy per chain in the brush is then presented as[12]

$$\frac{F}{F_{linear}} = \begin{cases} \eta^{2/3} & \upsilon \gg w\phi \\ \eta & \mid \upsilon \mid \ll w\phi \\ \eta^2 & \upsilon \leq 0, \mid \upsilon \mid \gg w\phi \end{cases} \quad (9)$$

where the last line in eq 9 describes only the elastic contribution to the total free energy per chain.

3 Brushes of Y-shaped polymers

The simplest case of a branched macromolecule is an Y-shaped polymer with the stem composed of n_1 monomer units and two branches with n_2 and n_3 ($n_3 \geq n_2$) monomer units emanating from a single branching point. Such polymer can be envisioned as a comblike polymer with one branching point or, equivalently, as an asymmetric starlike macromolecule with $q = 2$ free branches, **Figure 1**a.

As it is demonstrated in the Appendix, the self-consistency of the molecular potential in eq 1 in this case is attained if the topological coefficient κ is given by the minimal root of the equation

$$\tan(\kappa n_1)[\tan(\kappa n_2) + \tan(\kappa n_3)] = 1 \quad (10)$$

In a symmetric case, $n_1 = n_2 = n_3 = n$, the solution of eq 10 yields $\kappa = n^{-1}a\tan(1/\sqrt{2})$ to give $\eta = 3a\tan(1/\sqrt{2})$, a known result for a brush of end-tethered symmetric stars, $\eta = (q+1)a\tan(1/\sqrt{q})$, with $q = 2$. Notably, the solution of eq 10 can be found numerically for arbitrary values of n_1, n_2 and n_3. However, as we demonstrate below, it does not ensure the absence of dead zones (regions depleted of the free chain ends) and thus applicability of the parabolic molecular potential even in a planar geometry.

3.1 Numerical SF-SCF calculations for brushes of Y-shaped polymers.

The Scheutjens-Fleer self-consistent field method (SF-SCF) was used earlier to analyze the organization of brushes formed by star-like polymers.[9] The details about SF-SCF method can be found elsewhere.[16] Here we apply good (athermal) solvent conditions, $\chi = 0$, under which the effect of repulsive monomer-monomer interactions in the brush of branched macromolecules is maximal. In the parabolic molecular potential $U(z)$, the polymer density profile $\varphi(z)$ in a good solvent is expected to be parabolic as well provided that $\varphi(z) \ll 1$ (eq 4, first line).

Below, we focus on analyzing the shape of self-consistent potential (more particularly, its deviation from the expected parabolic shape) and distribution of free ends of both branches and branching points in brushes formed by Y-shaped polymers with systematically and independently varied DPs of the stem, n_1 and both free branches, n_2 and n_3.

As a reference system we use the brush formed by symmetric Y-shaped polymers with $n_2 = n_3$ and $N = n_1 + n_2 + n_3 = 300$ grafted to a planar surface with the density $\theta = Na^2/s = 5$. By plotting in **Figure 2**, the self-consistent potential is plotted as a function of z^2, we show that upon variation of the length of the stem $n_1 = N - (n_2 + n_3)$ in the range of $100 \leq n_1 \leq 200$, the profile of the self-consistent potential remains parabolic while the distributions of the free ends of both branches are unimodal and exhibit no dead zone proximal to the surface. For very short stem length, $n_1 = 2$, the branching points are located proximal to the grafting surface and the brush of symmetric Y-shaped polymers is equivalent to conventional monodisperse brush formed by linear chains with DP $n_2 = n_3$. The parabolic approximation is exact for such brushes as well. In the intermediate case of $n_1 = 40$ both distributions of the branching and end points exhibit a plateau shape which points to the onset of bimodal distributions of branching and end points. Such bimodal distributions are typical for stratified dendron brushes where the stems are strongly stretched in the non-linear elasticity regime.[31]

Let us now consider the effect of the branch bidispesity (asymmetry of branching) in brushes of Y-shaped macromolecules.

As demonstrated in the upper line in Figure 2, the asymmetry of branches does not perturb the parabolic shape of the self-consistent potential and does not lead to appearance of dead zones (depleted of the ends of longer branches) as long as the DP of the stem is sufficiently large (i.e., $n_1 = 200$). The distributions of the ends of long and short branches are close to each other and both retain unimodal shape while the distribution of the branching points is virtually unaffected by assymetry of branches.

For Y-shaped polymer with a constant degree of polymerization, N, and a long stem of $n_1 \geq N/3$ monomeric units, the self-consistent potential in the body of the brush is almost perfectly parabolic even if the branches become asymmetric, i.e., $n_2 \leq n_3$, and the cumulative end-points distribution splits into two modes corresponding to the shorter and to the longer branch, respetively.

The effect of branching asymmetry on the brush structure gets more pronounced upon a decrease in the DP n_1 of the stem (and concomitant increase in total DP of branches $n_2 + n_3$). At $n_1 = 100$ distributions of the ends of long and short branches only partially overlap though without

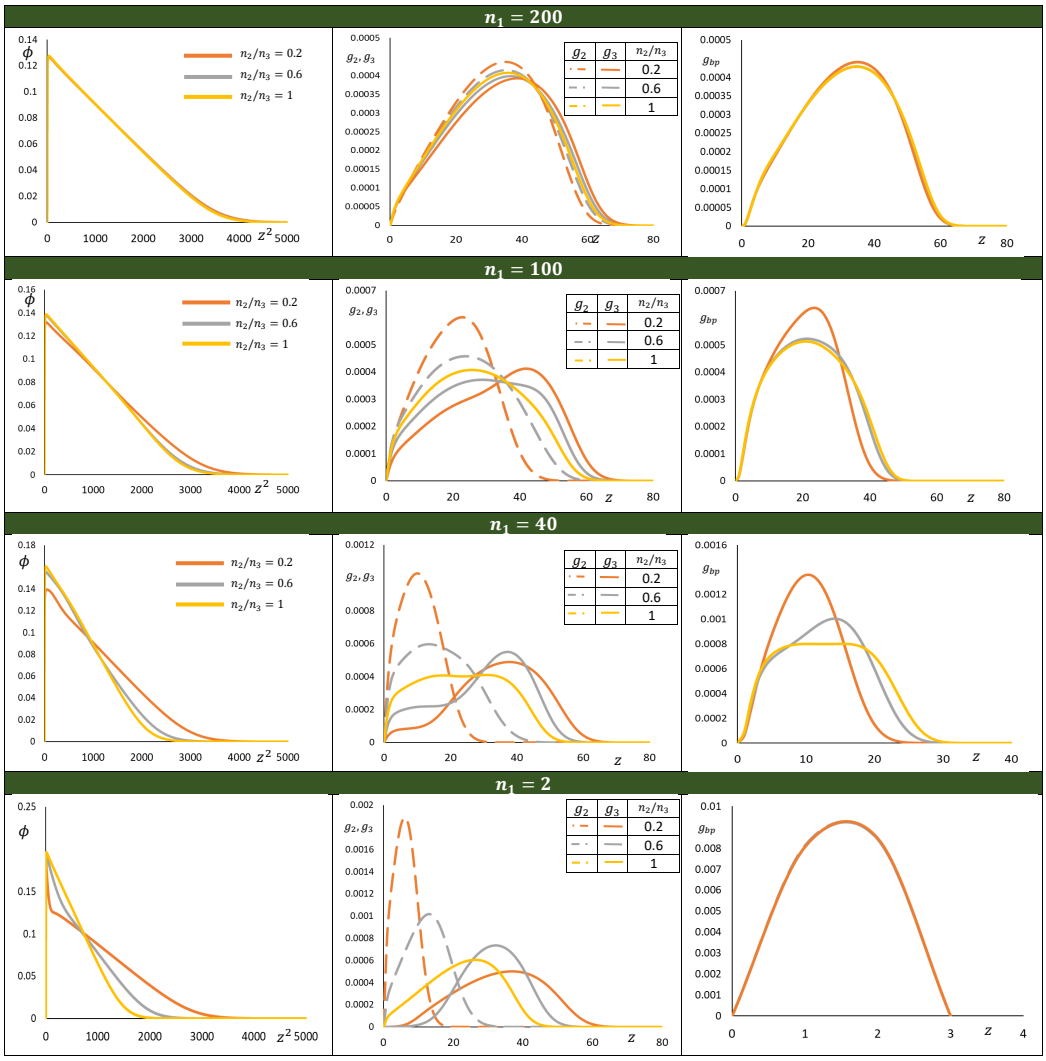

Figure 2: Self-consistent potential (left), free ends distributions (middle) and branching points distribution (right) in brushes of Y-shaped polymers, calculated numerically by SF-SCF method. The DP of the Y-shaped polymers $N = 300$ is kept constant, the DP of the stem n_1 is varied from 200 to 2, $n_2 \leq n_3$ are the DPs of branches.

pronounced dead zone. However, the apparent shoulder in the distribution of the longer branch ends indicates approaching onset of their depletion in the region proximal to the grafting surface and enrichment in the distal region of the brush. The branching point distribution remains unimodal, but its maximum is displaced towards grafting surface upon increasing branching asymmetry.

These trends become and even more pronounced for Y-polymers with shorter stem, $n_1 = 40$. The distribution of the ends of longer branch demonstrates pronounced depletion near the grafting surface, where the self-consistent potential strongly deviates from the parabolic shape. Notably, as discussed above, at $n_1 = 40$, the stem approaches the non-linear elasticity regime and the brush structure is affected by both asymmetry of branching and stratification. Here the parabolic shape of the self-consistent potential is strongly violated.

At vanishing stem length, the brush of asymmetric Y-shaped polymers becomes equivalent to a bidisperse brush of linear chains[14] with two different DPs, n_2 and n_3, and virtually non-overlapping end-point distributions of short and long chains: the ends of the longer chains are depleted from the proximal to the grafting surface region where short chains and their end points are located.

4 Brushes of comb-shaped polymers

4.1 Architecture of comb-shaped polymers

A comb-shaped polymer consists of P repeat units each comprising the main chain segment (spacer) with m_i monomer units ($i = 1, 2, ...P$) and $q_i \geq 1$ side chains each with n_{ij} monomers ($j = 1, 2, ...q_i$) linked to a single branching point on the main chain (backbone), see **Figure 1**b. If $q_i > 1$, such macromolecules are usually refered to as "barbwire" bottlebrushes.

The first backbone segment attached to the surface (the stem) has m_1 monomer units. The backbone has

$$M = \sum_{i=1}^{P} m_i \tag{11}$$

monomer units whereas total number of monomer units in one macromolecule is

$$N = \sum_{i=1}^{P} m_i + \sum_{i=1}^{P} \sum_{j=1}^{q_i} n_{ij} \tag{12}$$

4.2 Topolgical coefficient κ for comb-shaped polymers.

A scheme to calculate the topological coefficient κ and topological ratio $\eta = 2kN/\pi$ for a brush composed of comb-shaped macromolecules is described in details in ref[30] Here, we present only basic equations.

The topological coefficient κ can be found for abitrary set of parameters $\{m_i; n_{ij}\}$ and arbitrary P as a minimal root of the equation

$$\det \mathbf{A}_P = 0 \tag{13}$$

where matrix $\mathbf{A}_P$ is defined as

$$\mathbf{A}_P = \begin{pmatrix} -B_1(\kappa) & 1 & 0 & 0 & 0 & 0 \\ D_1(\kappa) & -B_2(\kappa) & 1 & 0 & 0 & 0 \\ 0 & D_2(\kappa) & -B_3(\kappa) & \dots & 0 & 0 \\ 0 & 0 & \dots & \dots & 1 & 0 \\ 0 & 0 & 0 & D_{P-2}(\kappa) & -B_{P-1}(\kappa) & 1 \\ 0 & 0 & 0 & 0 & -1 & C_P(\kappa) \end{pmatrix} \tag{14}$$

and its elements are related to parameters $\{m_i; n_{ij}\}$ as

$$B_i(\kappa) = \cos(\kappa m_{i+1}) + \frac{\sin(\kappa m_{i+1})}{\tan(\kappa m_i)} - \sin(\kappa m_{i+1}) \sum_{j=1}^{q_i} \tan(\kappa n_{ij}), i = 1, 2, .., P-1 \tag{15}$$

$$D_{i-1}(\kappa) = \frac{\sin(\kappa m_{i+1})}{\sin(\kappa m_i)}, i = 2, 3, ...P-1 \tag{16}$$

$$C_P = \cos(\kappa m_P) - \sin(\kappa m_P) \sum_{j=1}^{q_P} \tan(\kappa n_{Pj}) \tag{17}$$

Importantly, as we shall demonstrate below, the existence of the solution of eq 13 does not guarantee the parabolic shape of the self-consistent molecular potential.

The outlined above formalism provides a route to calculate the topological coefficient κ for macromolecules with a variety of comb-like architectures. In ref[30] we focused below on a representative case of macromolecules with equal lengths of side chains, $n_{ij} = n$, and equal branching activity of all the branching points, $q_i = q$. These macromolecules have

$$M = m_1 + (P-1)m \tag{18}$$

monomer units in the backbone, and total number of monomer units

$$N = M + Pqn = (m_1 - m) + P(m + qn) \tag{19}$$

The condition $m_1 \neq m_i, i = 2, 3, ...P$ is most essential for deviation of the molecular potential from the parabolic shape.

The topological coefficient κ can be related to the topological ratio η , as

$$\kappa = \frac{\pi\eta}{2N} = \frac{\pi\eta}{2M} \cdot \begin{cases} (1+qn/m)^{-1}, & m_1 = m \\ [1+qn/m+(m_1/m-1)/P]^{-1}, & m_1 \neq m \end{cases} \tag{20}$$

The asymptotic dependence for the topological ratio for such comb-shaped macromolecule can be obtained by assuming that the elastic stress propagates only through the main chain (backbone) of the macromolecule and reads

$$\eta \approx \frac{\kappa}{\kappa_{linear}} = \frac{2\kappa N}{\pi} = (1+qn/m)^{1/2} \approx (qn/m)^{1/2}, qn/m \gg 1 \tag{21}$$

which coincides with asymptotic numerical solution of eq 13, as discussed in ref[30]

4.3 SF-SCF results for comb-shaped polymers

Below we present the results of SF-SCF calculations for comb-shaped macromoelcules with $m_i = n_{ij} = n$, $q_1 = q_2 = ... = q_{P-1} = q$ and $q_P = q + 1$. For this architecture the total degree of polymerization is given by

$$N = n(1 + P + qP)$$

and the topological ratio is

$$\eta \approx \left(1 + \frac{qP}{P+1}\right)^{1/2}$$

The macromolecules are tethered to an impermeable planar surface with area s per chain. The grafting density $\theta = Na^2/s \geq 1$ ensures strong overlap of individual macromolecules and predominance of intermolecular interactions over intramolecular ones (the brush regime). The Flory-Huggins parameter for both main and side chains is set as $\chi = 0$, that corresponds to good (athermal) solvent conditions. In contrast to Y-shaped polymer, comb-shaped macromolecule with relatively small number of periods, P, demonstrate surprising features .

In **Figures 3a,b** , we present the polymer density profiles $\varphi(z)$ and $\varphi(z^2)$ in planar brushes of comb-shaped macromolecules with $m_i = n_{ij} = n = 100$, $q = 5$, fixed surface coverage $\theta = Na^2/s = (1 + P + Pq)a^2n/s = 20$, and varying P from $P = 1$(starlike polymer) to $P = 10$ (values of P are indicated near the curves). Variations in P at fixed surface coverage θ correspond to variations in the grafting area per macromolecules as $s/a^2 = (1+P+qP)n/\theta$.

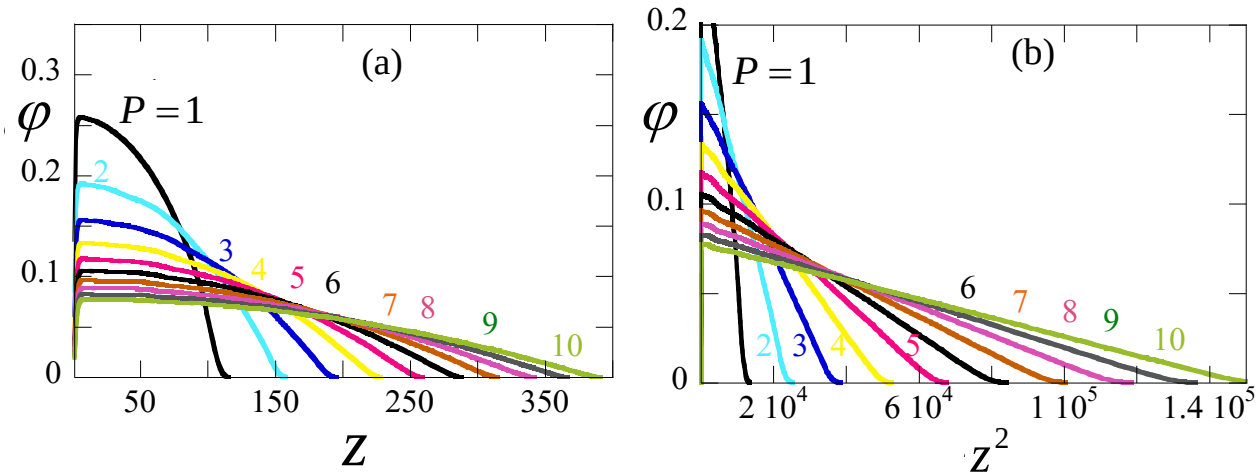

Figure 3: Polymer density profiles φ as a function of z (a) and z^2 (b) in planar brush of comb-shaped macromolecules with $m_0 = m = n$ and total number of monomer units $N = n + P(q+1)n$ at fixed surface coverage $Na^2/s = 20$. Other parameters are $m = n = 100$, $q = 5$, number of periods $P = 1, 2, 3, , 10$ indicated at the curves. The Flory-Huggins parameter $\chi = 0$.

As expected, at values of $\varphi(z) \lesssim 0.15$, polymer density profiles $\varphi(z^2)$ constitute almost perfect straight lines with conventional deviations at the brush edge and near the grafting surface. At larger values of $\varphi(z) > 0.15$, the profiles $\varphi(z^2)$ become slightly convex, which is can be explained by larger polymer concentration and contributions of higher order monomer-monomer interactions.

In **Figure 4** , we present the distributions $g(z)$ of the backbone endpoints for the same values of the parameters as in Figure 3. Surprisingly, distributions $g(z)$ demonstrate fine structure with numerous extrema in spite of remarkably simple density profiles in Figure 3. Starlike polymer ($P = 1$) with $q + 1 = 6$ free branches exhibits a smooth distribution of the branching monomer units (stem ends), pointing at a single population of moderately stretched stars. Segregation of starlike polymers within the brush into two populations with weakly and stongly stretched stems, respectively, is known to occur at higher grafting densities in the nonlinear elasticity regime.[9] In contrast, distribution $g(z)$ for comb-shaped macromolecules with $P = 2$ demonstrates two distinctive peaks indicating segregation of these macromolecules in two populations. Notably, this segregation occurs in the regime of Gaussian elasticity. Further increase in $P = 2, 3, 4$ leads to an increase in the number of peaks in $g(z)$ pointing at the presence of P distinctive populations of the tethered bottlebrushes. At $P > 5$ the fine structure of $g(z)$ smears and gradually disappears. No dead zones are found near the grafting surface, however, the depletion minimum in $g(z)$ in the vicinity of $z \simeq 50$ (i.e., at approximately half counter length of the stem) deepens with increasing P.

To examine the behavior of this depletion in more detail we increased the length n of the side chains with the simulteneous decrease in spacer length m, surface coverage θ, and increase in the number of periods P. In **Figures 5, 6**, we present polymer density profiles $\varphi(z)$ and backbone endpoint distributions $g(z)$ for $m_i = 50, n_{ij} = 200, q_i = 5 + \delta(P - i)$, and $\theta = 5$. Comparison of Figures 5 and 4 indicates that fine structure of $g(z)$ and the trend in its evolution observed upon an increase in P are retained. However, the relative contribution of the depleted zone in the total endpoint distribution, $g(z)$, decreases upon an increase in P, suggesting that for macromolecules with long backbone, $m_1 \simeq m$, and $P \gg 1$, the depletion effect could be neglected.

In **Figure 6**, the number of periods P increases up to $P = 80$. The evolution of distributions $g(z)$ upon an increase in P indicates further decrease of the depth of the minimum, its shift to smaller values of z, and final disappearance leading to perfectly smooth $g(z)$ at values of $P \gtrsim 60$.

A decrease in length m_1 of the stem (first spacer) leads to strong devia-

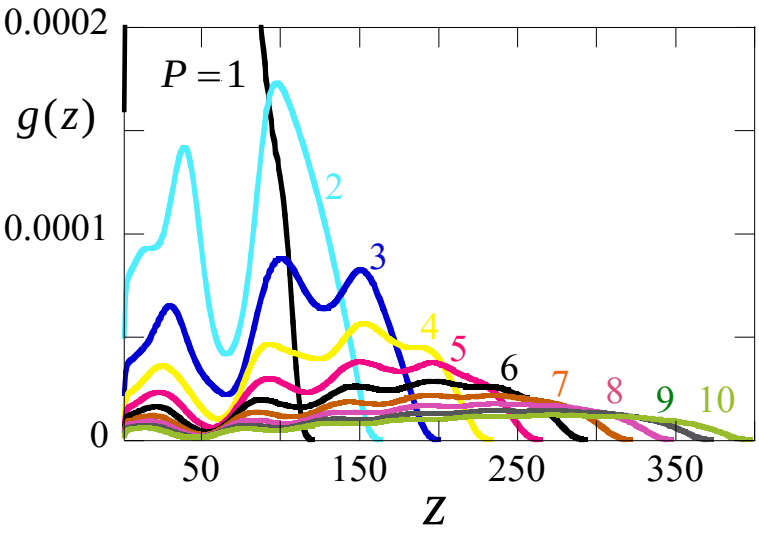

Figure 4: Distribution of the free ends of the backbone $g(z)$ in planar brush of comb-shaped macromolecules with $m_0 = m = n$ and total number of monomer units $N = n + P(q+1)n$ at fixed surface coverage $Na^2/s = 20$. Other parameters are $m = n = 100$, $q = 5$, number of periods $P = 1, 2, 3, , 10$ indicated at the curves. The Flory-Huggins parameter $\chi = 0$.

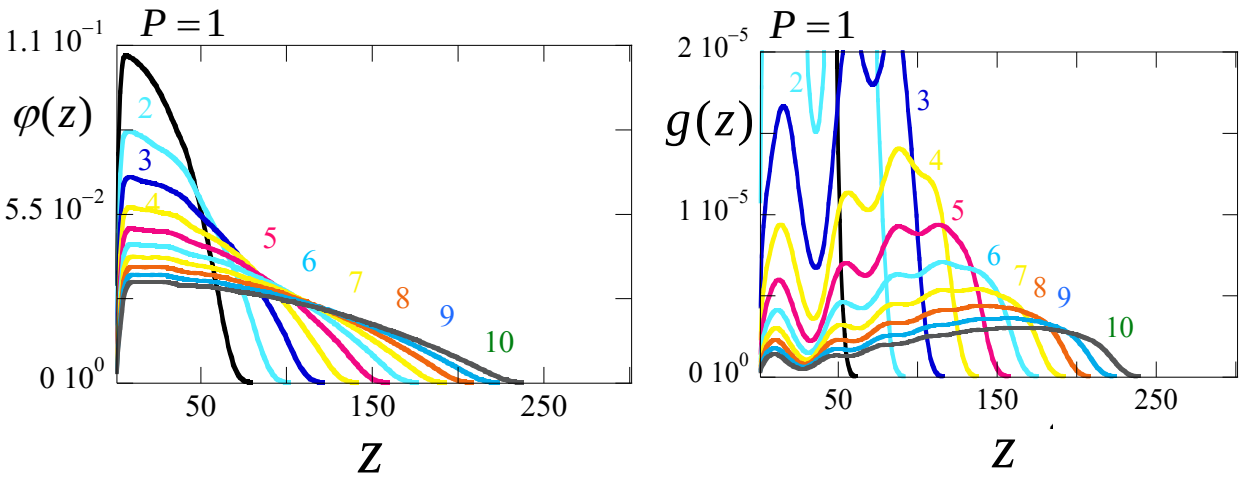

Figure 5: Polymer density profiles $\phi(z)$ and distribution of the free ends of the backbone $g(z)$ in planar brush of comb-shaped macromolecules with stem length $m_0 = m$ and total number of monomer units $N = m + P(qn + m)$ at fixed surface coverage $Na^2/s = 20$. Other parameters are $m = 50, n = 200, q = 5$, number of periods $P = 1, 2, 3, , 10$ indicated at the curves. The Flory-Huggins parameter $\chi = 0$.

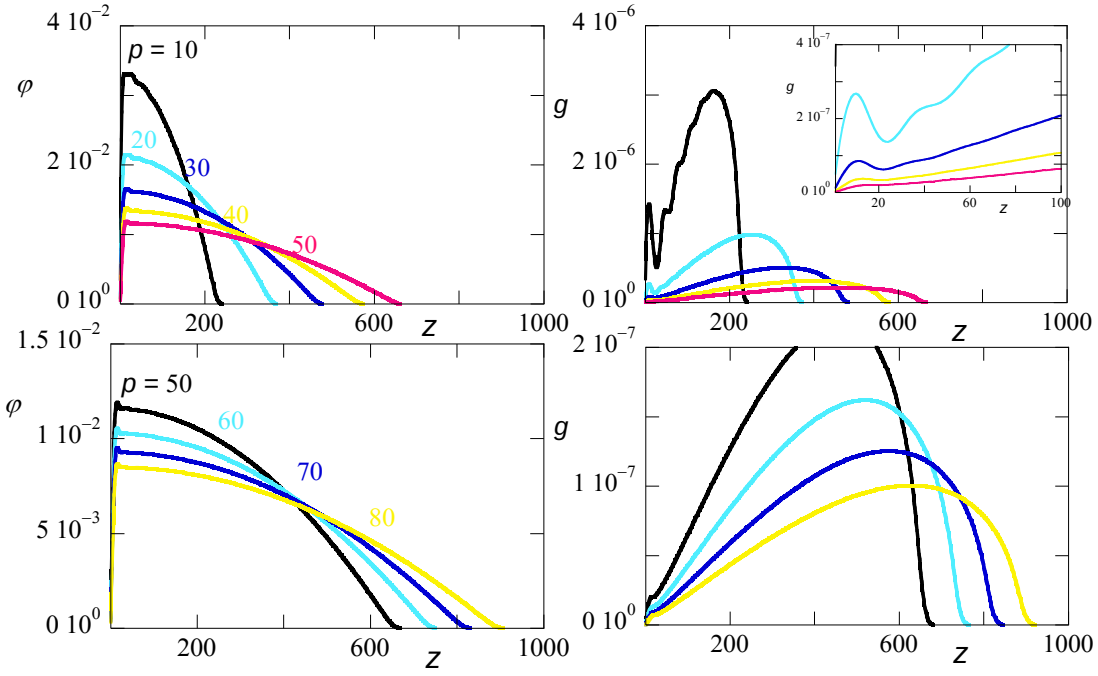

Figure 6: Polymer density profiles $\phi(z)$ and distribution of the free ends of the backbone $g(z)$ in planar brush of comb-shaped macromolecules with stem length $m_0 = m$ and total number of monomer units $N = m + P(qn + m)$ at fixed surface coverage $Na^2/s = 20$. Other parameters are $m = 50, n = 200, q = 5$, number of periods $P = 10, , 80$ indicated at the curves. The Flory-Huggins parameter $\chi = 0$.

tions of polymer density profile $\varphi(z)$ from the parabola. The shape of $\varphi(z)$ resembles the polymer density distribution in a two-component brush of linear polymers in which side chains emanating from the first branching point constitute one component while the rest of the bottlebrush - the second component. In accord with this picture, the "dead zone" free of the backbone ends (i.e. with $g(z) = 0$) develops near the surface.

In **Figure 7** we present the polymer density profiles $\varphi(z)$ and distributions of the backbone end-point, $g(z)$, for macromolecules without a stem, $m_1 = 0$, that illustrate these features: complex (nonparabolic) shape of $\varphi(z)$ and dead zone with $g(z) = 0$ near the grafting surface .

However, the trends found in the case of $m_1 = m$ hold for $m_1 = 0$ as well. That is, an increase in P leads to gradual transformation of the polymer density profile in the parabola, and disappearance of both depletion in the vicinity of $z \simeq 50$, and dead zone near the surface.

5 Discussion and conclusions

In this study we have examined the applicability of the parabolic self-consistent potential approximation for planar brushes formed by macromolecules with branched architectures different from that of linear chains or regular dendrons. In the latter two cases, the parabolic approximation is known to be exact in the limit of linear conformational elasticity of the brush-forming macromolecules. For branched macromolecules with less regular architecture, the topological parameter of the parabolic potential can be calculated within SS-SCF scheme as well though this route does not provide a proof of self-consistency of the parabolic potential. We applied numerical SF-SCF scheme to calculate true self-consistent potential which appears to deviate from parabolic shape for such simple architectures as asymmetric Y-shaped and comb-shaped polymers with short stems. The deviation of the self-consistent potential from the parabola is accompanied by peculiar patterns in the free ends distribution functions.

Hence, the results of our study demonstrates that although topological coefficient in the parabolic potential can be routinely calculated for any branched polymer architecture, this calculation does not provide itself an unambigious proof of applicability of the SS-SCF analytical scheme to brushes formed by arbitrary tree-like macromolecules.

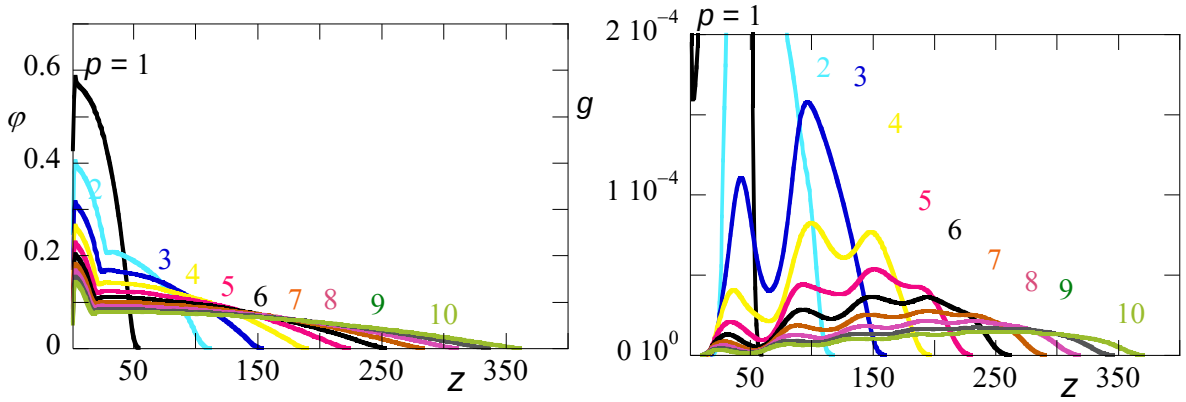

Figure 7: Polymer density profiles $\phi(z)$ and distribution of the free ends of the backbone $g(z)$ in planar brush of comb-shaped macromolecules with stem length $m_0 = 0$ with total number of monomer units $N = P(q+1)n$ at fixed surface coverage $\theta = Na^2/s = 20$. Other parameters are $m = n = 100$, $q = 5$, number of periods $P = 1, , 10$ indicated at the curves. The Flory-Huggins parameter $\chi = 0$.

Appendix: self-consistent potential for brushes of Y-shaped macromolecules

Below we demonstrate how a self-consistent parabolic molecular potential

$$U(z) = U(0) - \frac{3}{2a^2}\kappa^2 z^2 \tag{22}$$

(measured in k_BT units) with specifically tailored coefficient κ ensures independence of the free energy penalty Ω for insertion of a probe Y-shaped polymer (depicted in Figure 1).

In the strong stretching approximation (SSA), the chain conformations in the self-consistent or external potential field are described via trajectories that specify the most probable position of each monomer unit at given position of the chain end-point. We introduce the trajectory and stretching functions of the stem, $E_0(z) = dz/dj$, and corresponding branches, $E_1(z)$ and $E_2(z)$ for the Y-shaped polymer with specified positions $z = y_1$ and $z = y_2$ of the ends of the shorter and the longer free branches, respectively.

If tethered to the surface Y-shaped polymers is subjected to external potential $U_{ex}(z)$, then the free energy of such polymer (measured in k_BT units) can be presented as

$$\Omega = \int_0^{z_1} \left[\frac{3}{2a^2}E_0(z) + \frac{U_{ex}(z)}{E_0(z)}\right] dz +$$

$$\int_{z_1}^{y_1} \left[\frac{3}{2a^1}E_1(z) + \frac{U_{ex}(z)}{E_1(z)}\right] dz + \int_{z_1}^{y_2} \left[\frac{3}{2a^2}E_2(z) + \frac{U_{ex}(z)}{E_2(z)}\right] dz \tag{23}$$

where the first, the second and the third integrals correspond to contributions of the stem, short and long free branches, respectively. The first term in each integral accounts for the elastic (conformational) free energy, whereas the second term is the energy of the corresponding chain segment (stem or free branch) in the potential $U_{ex}(z)$.

The stretching functions E_0, E_1, E_2 of the chain segments, and the position z_1 of the branching point can be derived by minimization of the free energy given by eq 23 with the account of conservation of the numbers of monomer units in each segment of the Y-shaped macromolecule, that is,

$$\int_0^{z_1} \frac{dz}{E_0(z)} = n_0; \int_{z_1}^{y_1} \frac{dz}{E_1(z)} = n_1; \int_{z_1}^{y_2} \frac{dz}{E_2(z)} = n_2 \tag{24}$$

which is reduced to the minimization of the functional

$$\Phi = \int_0^{z_1} \left[\frac{3}{2a^2}E_0(z) + \frac{U_{ex}(z) + \lambda_0}{E_0(z)}\right] dz +$$

$$\int_{z_1}^{y_1}\left[\frac{3}{2a^2}E_1(z)+\frac{U_{ex}(z)+\lambda_2}{E_1(z)}\right]dz+\int_{z_1}^{y_2}\left[\frac{3}{2a^2}E_2(z)+\frac{U_{ex}(z)+\lambda_1}{E_2(z)}\right]dz \quad (25)$$

The indefinite Lagrange multiplies λ_0, λ_1, and λ_2, insure the concervation of the number of monomers in each chain segment. Variation of functional Φ with respect to the unknown functions E_0, E_1, E_2 leads to the set of equations:

$$E_i(z)=\sqrt{\frac{2a^2}{3}}\sqrt{U_{ex}(z)+\lambda_i}, \qquad i=0,1,2 \quad (26)$$

Lagrange multiplies λ_1, and λ_2 are found from the condition of vanishing tension at free ends of the branches,

$$\lambda_i=-U_{ex}(y_i), \qquad i=1,2 \quad (27)$$

to give

$$E_0(z)=\sqrt{\frac{2a^2}{3}}\sqrt{U_{ex}(z)+\lambda_0} \quad (28)$$

$$E_1(z)=\sqrt{\frac{2a^2}{3}}\sqrt{U_{ex}(z)-U_{ex}(y_1)} \quad (29)$$

$$E_2(z)=\sqrt{\frac{2a^2}{3}}\sqrt{U_{ex}(z)-U_{ex}(y_2)} \quad (30)$$

With the account of eqs 28, 29, 30, functional Φ reduces to

$$\Phi\frac{a}{\sqrt{6}}=$$

$$\int_0^{z_1}\sqrt{U_{ex}(z)+\lambda_0}dz+\int_{z_1}^{y_2}\sqrt{U_{ex}(z)-U_{ex}(y_2)}dz+\int_{z_1}^{y_1}\sqrt{U_{ex}(z)-U_{ex}(y_1)}dz \quad (31)$$

The subsequent minimization of the functional Φ given by eq 31 with respect to z_1 leads to the equation,

$$\sqrt{U_{ex}(z_1)+\lambda_0}-\sqrt{U_{ex}(z_1)-U_{ex}(y_2)}-\sqrt{U_{ex}(z_1)-U_{ex}(y_1)}=0 \quad (32)$$

Notably, eq 32 is equivalent to the balance of elastic forces,

$$E_0(z_1)=E_1(z_1)+E_2(z_1)$$

in the branching point.

The application of normalization conditions given by eq 24 provides three equations,

$$\int_0^{z_1} \frac{dz}{\sqrt{U_{ex}(z)+\lambda_0}} = \sqrt{\frac{2a^2}{3}} n_0 \tag{33}$$

$$\int_{z_1}^{y_1} \frac{dz}{\sqrt{U_{ex}(z)-U_{ex}(y_1)}} = \sqrt{\frac{2a^2}{3}} n_1 \tag{34}$$

$$\int_{z_1}^{y_2} \frac{dz}{\sqrt{U_{ex}(z)-U_{ex}(y_2)}} = \sqrt{\frac{2a^2}{3}} n_2 \tag{35}$$

By substituting eqs 28 - 30, and 33 - 35 in eq 23, one finds the penalty for insertion of an Y-shaped polymer into the external field $U_{ex}(z)$

$$\Omega = 2\sqrt{\frac{3}{2a^2}} \left\{ \int_0^{z_1} \sqrt{U_{ex}(z)+\lambda_0} dz + \int_{z_1}^{y_1} \sqrt{U_{ex}(z)-U_{ex}(y_1)} dz + \int_{z_1}^{y_2} \sqrt{U_{ex}(z)-U_{ex}(y_2)} dz \right\} - \lambda_0 n_0 + U_{ex}(y_1) n_1 + U_{ex}(y_2) n_2 \tag{36}$$

We now show that if $U_{ex}(z)$ is given by eq 22 with the topological coefficient κ given by the minimal solution of equation

$$\tan(\kappa n_0)[\tan(\kappa n_2) + \tan(\kappa n_1)] = 1, \tag{37}$$

then the insertion free energy penalty Ω in eq 36 is independent of the position y_2 of the free end of the longest branch (or, equivalently, on positions y_1 or z_1 of the shorter branch or the branching point, respectively) of the Y-shaped polymer.

Substituting $U(z) = U_{ex}(z)$ given by eq 22 into eqs 28 - 30 leads to

$$E_0(z) = \sqrt{\frac{2a^2}{3}} \sqrt{U(0) + \lambda_0 - \frac{3}{2a^2}\kappa^2 z^2} \tag{38}$$

$$E_1(z) = \sqrt{\frac{2a^2}{3}} \sqrt{U(z) - U(y_1)} = \kappa \sqrt{y_1^2 - z^2} \tag{39}$$

$$E_2(z) = \sqrt{\frac{2a^2}{3}} \sqrt{U(z) - U(y_2)} = \kappa \sqrt{y_2^2 - z^2} \tag{40}$$

whereas substituting eq 22 into eqs 33 - 35 leads to

$$\sqrt{\frac{3}{2a^2}} \frac{z_1 \kappa}{\sqrt{U(0)+\lambda_0}} = \sin(\kappa n_0) \tag{41}$$

$$\frac{z_1}{y_1} = \cos(\kappa n_1) \tag{42}$$

$$\frac{z_1}{y_2} = \cos(\kappa n_2) \tag{43}$$

where eq 41 can be presented as

$$\lambda_0 + U(0) = \frac{3}{2a^2}\frac{z_1^2\kappa^2}{\sin^2(\kappa n_0)} \tag{44}$$

Eq 32 reduces to

$$\sqrt{U(0) + \lambda_0 - \frac{3}{2a^2}\kappa^2 z_1^2} - \sqrt{\frac{3}{2a^2}}\kappa\sqrt{y_1^2 - z_1^2} - \sqrt{\frac{3}{2a^2}}\kappa\sqrt{y_2^2 - z_1^2} - \tag{45}$$

and, finally, with the account of eqs 42 - 44

$$\sqrt{\frac{[U(0) + \lambda_0]2a^2}{3\kappa^2 z_1^2} - 1} = \sqrt{\frac{y_1^2}{z_1^2} - 1} + \sqrt{\frac{y_2^2}{z_1^2} - 1} \tag{46}$$

Substitution of eqs 42 - 44 in eq 46 leads to eq 37.

The relative positions of the free end of the shorter branch and of the branching point yield

$$y_1 = y_2\frac{\cos(\kappa n_2)}{\cos(\kappa n_1)}; z_1 = y_2\cos(\kappa n_2); \tag{47}$$

while the stretching function $E_0(z)$ is given by

$$E_0(z) = \kappa\sqrt{\frac{z_1^2}{\sin^2(\kappa n_0)} - z^2} \tag{48}$$

By using eqs 38, 39,40 and eq 44 into eq 36 the insertion free energy penalty of probe chain can be calculated as

$$\Omega = U(0)(n_1 + n_2 + n_3) = U(0)N \tag{49}$$

Hence, Ω does not depend on position y_2 of the free end of the inserted Y-shaped polymer. If the molecular potential acting on each monomer unit inside the brush is given by eq 22, then chain insertion free energy Ω given by eq 49 coincides with the chain chemical potential.

Whether for any given set of $\{n_1, n_2, n_3\}$ the potential given by eq 22 is really self-consistent can be proven only by numerical calculations which indicate absence of presence of the dead zone and provide the trueshape of the self-consistent potential. As demonstrated above, in spite of existing solution of eq 37, not for any set of $\{n_1, n_2, n_3\}$ the parabolic potential given by eq eq 22 is a self-consistent one.

Acknowledgment

This work was supported by Russian Science Foundation grant 20-13-00270

References

[1] Alexander, S. Adsorption of chain molecules with a polar head: a scaling description *J.Phys.(France)*, **1977**, *38*, 983-987.

[2] de Gennes P.-G. Conformations of Polymers Attached to an Interface *Macromolecules*, **1980**, *13*, 1069-1075.

[3] Semenov, A. N. Contribution to the theory of microphase layering in block copolymer melts. *Sov. Phys. JETP.* **1985**, *61*, 733-742.

[4] Zhulina E.B., Pryamitsyn V.A., Borisov O.V. Structure and Conformational Transitions in Grafted Polymer Chains Layers: New Theory. *Polym.Sci.USSR* **1989**, *31*, 205-215.

[5] Milner, S.T.; Witten, T.A.; Cates, M.E. Theory of the grafted polymer brush. *Macromolecules* **1988**, *21*, 2610.

[6] Birshtein, T.M., Amoskov, V.M. Polymer brushes. *Polym.Sci. C* **2000**, *42*, 172-213

[7] Pickett G. T. Classical Path Analysis of end-Grafted Dendrimers: Dendrimer Forest. *Macromolecules* **2001**, *34*, 8784–8791.

[8] Zook, T. C.; Pickett, G. T. Hollow-Core Dendrimers Revised. *Physical review letters***2003**, *90(1)*, 015502.

[9] Polotsky, A. A.; Leermakers, F. A. M.; Zhulina, E. B.; Birshtein, T. M. On the Two-Population Structure of Brushes Made of Arm-Grafted Polymer Stars. *Macromolecules* **2012**, *45*, 7260–7273.

[10] Zhulina, E. B.; Leermakers, F. A. M. ; Borisov O.V. Theory of brushes formed by Ψ-shaped macromolecules at solid-liquid interfaces. *Langmuir* **2015,***31* (23), 6514–6522

[11] Zhulina, E. B. ; Leermakers, F. A. M.; Borisov O.V. Ideal mixing in multicomponent brushes of branched macromolecules. *Macromolecules* **2015**,*48* (23), 5614–5622

[12] Lebedeva, I.O.; Zhulina, E. B. ; Leermakers, F. A. M.; Borisov O.V. Dendron and Hyperbranched Polymer Brushes in Good and Poor Solvents. *Langmuir* **2017**,*33*, 1315-1325

[13] Zhulina, E. B. ; Leermakers, F. A. M.; Borisov O.V. Brushes of Cycled Macromolecules: Structure and Lubricating Properties. *Macromolecules* **2016**,*49* (22), 8758–8767

[14] T.M. Birshtein, Yu.V. Liatskaya and E.B. Zhulina, *Polymer*, 1990, **31**, 2185 - 2196.

[15] S. Qi, S.; Klushin, L.I.; A. M. Skvortsov, A.M.; Schmid, F. Polydisperse Polymer Brushes: Internal Structure, Critical Behaviour and Interaction with Flow. *Macromolecules*, 2016, **49**, 9665–9683.

[16] Fleer, G.J.; Cohen Stuart, M.A.; Scheutjens, J.M.H.M.; Cosgrove, T.; Vincent, B. *Polymers at Interfaces*, Chapman & Hall, London, 1993

[17] Li,C.-W.; Merlitz,H.; Wu, C.-X.; Sommer, J.-U. The structure of brushes made of dendrimers: Recent advances *Polymer* **2016**, *98*, 437-447

[18] J. Rzayev Synthethis of polystyrene-polylactide bottlebrush block copolymers and their melt self-assembly into large domain nanostructures. *Macromolecules* **2009**, *42*, 2135-2141

[19] Liberman-Martin, A.L.; Chu, C.K.; Grubbs, R.H. Application of Bottlebrush Block Copolymers as Photonic Crystals. *Macromol.Rapid.Comm.* **2017**, *38*, 1700058

[20] Song, D.P.; Zhao, T.H.; Guidetti, G.; Vignolini, S.; Parker, R.M. Hierarchical Photonic Pigments via the Confined Self-Assembly of Bottlebrush Block Copolymers. *ACS Nano* **2019**, *13*, 1764-1771.

[21] M. Vatankhah-Varnosfaderani, A.N. Keith, Y. Cong, H. Liang, M. Rosenthal, M. Sztucki, C. Clair, S. Magonov, D.A. Ivanov, A. V. Dobrynin, S.S. Sheiko. Chameleon-like elastomers with molecularly encodded strain-adaptive stiffening and coloration. *Science* **2019**, 359, 1509-1513.

[22] J. Bolton, T.S. Baile, J. Rzayev. Large pore size nanoporous materials from self-assembly of asymmetric bottlebrush block copolymers. *Nano Lett.* **2011**, *11*, 998-1001

[23] Y. Gai, D.-P. Song, B. M. Yavitt, J. J. Watkins. Polystyrene-block-poly(ethylene oxide) Bottlebrush Block CopolymerMorphology Transitions: Influence of Side Chain Length and Volume Fraction. *Macromolecules* **2017**, *50*, 1503-1511

[24] M.B. Runge, N.B. Bowden. Synthesis of High Molecular Weight Comb Block Copolymers and Their Assembly into Ordered Morphologies in the Solid State. *JACS* **2007**, *129*, 10551-10560

[25] M.B. Runge, C.E. Lipscomb, L.R. Ditzler, M.K. Mahanthappa, A.V. Tivanski, N.B. Bowden. Investigation of the Assembly of Comb Block Copolymers in the Solid State. *Macromolecules* **2008**, *41*, 7687-7694

[26] H.-F. Fei, B. M. Yavitt, X. Hu, G. Kopanati, A. Ribbe, J. J. Watkins.Influence of Molecular Architecture and Chain Flexibility on the Phase Map of Polystyrene-block-poly(dimethylsiloxane) Brush Block Copolymers. *Macromolecules* **2019**, *52*, 6449-6457

[27] D.F. Sunday, A. B. Chang, C. D. Liman, E. Gann, D. M. Delongchamp, L. Thomsen, M. W. Matsen, R. H. Grubbs, C. L. Soles. Self-Assembly of ABC Bottlebrush Triblock Terpolymers with Evidence for Looped Backbone Conformations. *Macromolecules* **2019**, *52*(4), 1557-1566

[28] J. Bolton, J. Rzayev. Synthesis and Melt Self-Assembly of PS-PMMA-PLA Triblock Bottlebrush Copolymers. *Macromolecules* **2014**, 47, 2864-2874

[29] Rud, O.V., Polotsky, A.A.; Gillich, T.; Borisov, O.V.; Leermakers, F.A.M.; Textor, M.; Birshtein, T.M. Dendritic Spherical Polymer Brushes: Theory and Self-Consistent Field Modelling. *Macromolecules* **2013**, *46*, 4651-4662

[30] Zhulina, E.B.; Mikhailov, I.V.; Borisov, O.V. Brushes and lamellar mesophases of comb-shaped (co)polymers: a self-consistent field theory. *Physical Chemictry Chemical Physics* **2020**, *22* (40), 23385–23398

[31] Borisov, O. V. ; Polotsky, A. A.; Rud, O. V.; Zhulina, E. B.; Leermakers, F. A. M.; Birshtein, T. M. Dendron Brushes and Dendronized Polymers: A Theoretical Outlook. *Soft Matter* **2014**, *10*, 2093-2101.